Effect of fluid medium on mechanical behavior of carbon nanotube foam

Abha Misra, Praveen Kumar, Jordan R. Raney, Anish Singhal, Ludovica Lattanzi, and Chiara Daraio

Citation: Applied Physics Letters **104**, 221910 (2014); doi: 10.1063/1.4881843
View online: http://dx.doi.org/10.1063/1.4881843
View Table of Contents: http://scitation.aip.org/content/aip/journal/apl/104/22?ver=pdfcov
Published by the AIP Publishing

Effect of fluid medium on mechanical behavior of carbon nanotube foam

Abha Misra,[1] Praveen Kumar,[2] Jordan R. Raney,[3] Anish Singhal,[1] Ludovica Lattanzi,[4] and Chiara Daraio[4,5,a)]
[1]*Department of Instrumentation and Applied Physics, Indian Institute of Science, Bangalore, Karnataka 560012, India*
[2]*Department of Materials Engineering, Indian Institute of Science, Bangalore, Karnataka 560012, India*
[3]*Department of Mechanical Engineering, Baylor University, Waco, Texas 76798, USA*
[4]*Division of Engineering and Applied Science, California Institute of Technology, Pasadena, California 91125, USA*
[5]*Department of Mechanical and Process Engineering, ETH Zürich, Zürich CH-8092, Switzerland*

(Received 7 November 2013; accepted 26 May 2014; published online 6 June 2014)

This study reports the constitutive response and energy absorption capabilities of fluid-impregnated carbon nanotube (CNT) foams under compressive loading as a function of fluid viscosity and loading rates. At all strain rates tested, we observe two characteristic regimes: below a critical value, increasing fluid viscosity increases the load bearing and energy absorption capacities; after a critical value of the fluid's viscosity, we observe a rapid decrease in the systems' mechanical performance. For a given fluid viscosity, the load bearing capacity of the structure slightly decreases with strain rate. A phenomenological model, accounting for fluid-CNT interaction, is developed to explain the observed mechanical behavior. © *2014 AIP Publishing LLC*. [http://dx.doi.org/10.1063/1.4881843]

The ability to fabricate large quantities of carbon nanotube (CNT) foam or cellular structures at affordable costs has made these materials quite attractive for several engineering applications, ranging from structural to functional.[1] Several studies have been carried out to reveal the mechanical properties of bulk CNT foams.[2–15] CNT foams have been shown to combine lightweight, high porosity, and large surface area with relatively high stiffness and tunable energy absorption capacity.[4,16,17] Recently, CNT foams have been assembled into multilayer structures presenting superior energy absorption capability as compared to other conventional layered, metallic and polymeric foams and fibrous cushioning materials.[17,18] Therefore, there is a general consensus that CNT and CNT-based materials possess superb potential to be used as ideal materials for cushioning and impact damping,[1–3,7] providing orders of magnitude higher energy absorption per unit volume (and weight) as compared to conventional cushioning materials.[4,9] In addition, the bulk properties of CNT foams have also been suggested to be useful in a wide range of applications from acoustic, vibration, and impact mitigation[2,19,20] to lipophilic absorbent sponges.[21]

Earlier reports[22–24] have examined the mechanical behavior of open cell (reticulated) foams filled with Newtonian fluids, showing their better potential to absorb energy and impede shock waves. Here, we extend these studies to foam-like materials composed of aligned CNTs. We show that the quasi-static compressive response of aligned CNT structures can be tuned by fluid impregnation. For example, the selection of specific fluid viscosity can enhance the load carrying and energy absorbing capabilities of the CNT foams.

Although CNT foams have similar mechanical compressive characteristics as classical open cell foams,[7,25] less is known about the micro-structural effects influencing their overall mechanical response. For example, the role of van der Waals' interactions between adjacent CNTs, the rigidity of the nodes formed in the entanglement of multiple CNTs, and the role of imperfections are still not fully understood. This study employs fluids with varying viscosity to vary the CNT interactions and the resulting mechanical response of the bulk CNT structures.

The vertically aligned CNT foams used in our tests were synthesized using a chemical vapor deposition (CVD) reactor consisting of a one-meter long, 50 mm diameter quartz tube. Vapors of ferrocene and toluene solution were passed through the reaction zone at 827 °C. These vapors were carried to the reaction zone using argon as a carrier gas. Si wafers with $\sim 1\,\mu$m oxide film were used as growth substrates and positioned in the high temperature zone of the reactor. The CNT foams grew normal to the SiO_2 surface, forming vertically oriented bundles with a complex microstructure (more details of the CVD growth procedure can be found elsewhere[9]). The as-grown CNT samples ($\sim$2 mm thick) were removed from the substrate with a razor blade, and samples with cross-section of 2×2 mm^2 were cut using a sharp razor blade.

As shown in Figure 1(a), the microstructure of the as-grown CNT forests was highly entangled, resulting in a foam with high porosity. The bulk density of the CNT foams, ρ, was calculated by dividing their measured mass by the volume.[9] The relative density, ρ/ρ_s, where ρ_s is the density of a CNT, varied between 13% and 27%, similar to open cell foam structures (i.e., with a $\rho/\rho_s < 30\%$).[25] Based on the analysis of high magnification scanning electron microscope (SEM) images (such as Figure 1(a)), the mean pore size of the CNT foams was estimated to be $\sim 1\,\mu$m.

Figure 1(b) shows a schematic of the experimental setup employed to study the mechanical behavior of the CNT foam-fluid composite. A solid, flat platen of hardened steel was utilized to compress free-standing CNT foams. During

a)Author to whom correspondence should be addressed. Electronic mail: daraio@ethz.ch. Telephone: +41-446328946.

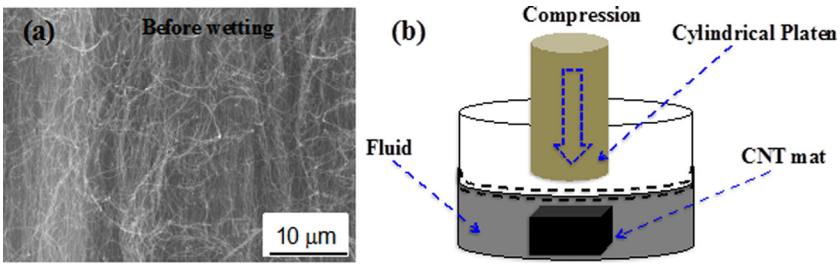

FIG. 1. (a) Representative SEM micrograph of the as-grown, dry CNT foam sample. (b) A schematic of the experimental setup used for compression measurement of the CNT with varying concentration of fluids.

testing, the foams were fully submerged into a water-glycerol solution with four different concentrations: 100, 80, 40, and 10 wt. % of glycerol, which correspond to viscosities of 612, 34, 2.72, and 1.03 mPa s, respectively, at room temperature.[26] Before testing, the CNT foams were soaked in the solutions for 24 h to ensure complete (or, a steady state) impregnation.

Quasi-static cyclic compression tests on the fluid-immersed CNT foams were performed using an Instron mechanical tester (E3000) under displacement-controlled mode. The CNT foams were compressed to a maximum strain of 50% at different engineering strain rates (0.3, 3, and 50% s^{-1}). Following compression, the unloading was also conducted at the same engineering strain rate. For the purpose of comparison, a few as-grown, dry CNT foams were also tested under the same experimental conditions. At least six different samples were tested under each test condition to verify repeatability and to ensure statistical accuracy.

Figure 2 shows typical stress-strain profiles of CNT foams wetted with water-glycerol solutions with various weight fractions of glycerol and at a few different strain rates. The plots include the results obtained by testing all six samples at each test condition. Figures 2(a), 2(c), and 2(e) show considerable scatter in the stress values at a given strain for different samples. The observed scatter can be attributed to the difference in densities of the various CNT foams tested.[9,27] As reported in an earlier study on the similar as-grown, dry CNT foams,[9] and CNT turfs,[27] the dependence of stress, σ, on the density, ρ, is nominally linear, i.e., $\sigma = \sigma_0 + k\rho$, where σ_0 and k are constants. As shown in Figures 2(b), 2(d), and 2(f), the scatter in the stress-strain graphs is dramatically reduced when the stress values are normalized by the density of the as-grown, dry CNT foam. Although the effective density of the CNT foam soaked in a liquid and subjected to compressive strain may differ from the as-grown dry state, normalization of stress by dividing it by the density of the as-grown, dry CNT foam proves to be an effective way of reducing the scatter arising from the sample to sample variation that is known to exist as a result of changes to CNT diameters. Therefore, even if it appears as the first order approximation, the density of the as-grown, dry CNT foam can be considered as the representative density of the liquid soaked CNT foams tested in this study.

As shown by Figures 2(b) and 2(d), the stress increased continuously without appearance of any distinctive plateau region when compressed at low strain rates (0.3 and 3.0% s^{-1}). The same behavior was generally observed for all fluid concentrations, except for samples tested at relatively high strain rate (3% s^{-1}) and wetted with a very high viscosity fluid ($\geq$80% glycerol). This monotonic stress-strain behavior is similar to what was also observed for the as-grown, dry, free-standing CNT foams tested in this study, as well as reported earlier,[16,28] clearly indicating that the typical deformation mechanism of a CNT foam did not change when wetted with low viscosity fluids, provided the samples were compressed at low strain rates. This might be explained by the fact that the low viscosity fluids, compressed at low loading rates, can be easily expelled from the pores of the structure without significantly affecting the deformation mechanism of the CNT foam.

Interestingly, as shown in Figure 2(f), the compression of CNT foam-fluid composite at high strain rate (50% s^{-1}) resulted in the formation of a distinct plateau in the stress-strain plots. This behavior was observed for all fluid viscosities tested. The fraction of the plateau region in the entire loading segment of the stress-strain profile increased with the viscosity. Such a behavior was not observed when testing as-grown, dry, freestanding CNT foams. Since the formation of a plateau region in classical foams indicates the collapse of struts and ligaments (which occurs without significant resistance), this behavior at high strain rate suggests that the liquid trapped inside the CNT foam might be responsible for a similar collapse of individual CNT cell, formed by crisscrossing CNT strands and nodes, in the foam structure. The probability of trapping liquid inside the deforming foams increases with strain rate. This finding will later be used to develop a phenomenological model for the mechanical behavior of the CNT foam-fluid composite.

Figure 3 is a contour plot showing the effect of the strain rate and the glycerol concentration (or, viscosity) on the maximum stress (i.e., at $\varepsilon = 50\%$). For the interpolation between the experimentally calculated data points, the Chebyshev 2D nonlinear surface curve fitting function of Origin® software was used. Figure 3 reveals that at any strain rate, the peak stress increases with glycerol concentration (or viscosity) up to a critical concentration value ($\sim$30%). After the critical value, the maximum stress monotonically decreases. The maximum load-bearing capacity of the CNT foam-fluid composite occurred when the loading rate was low and the viscosity of the fluid was moderate (glycerol concentration of $\sim$30%). The wetted CNTs dramatically lost the load bearing capacity when the loading rate was very high and the fluid had a high concentration of glycerol (Figure 3). The peak stress of CNT foam wetted with high concentrations of glycerol ($\geq$80%) was actually lower than even the as-grown, dry, free-standing CNT foams. It should be noted that the strain energy absorbed per loading cycle, calculated by measuring the area of the stress-strain hysteresis, showed a trend similar to the peak stress per cycle (or, load bearing capacity). Based on the above results and

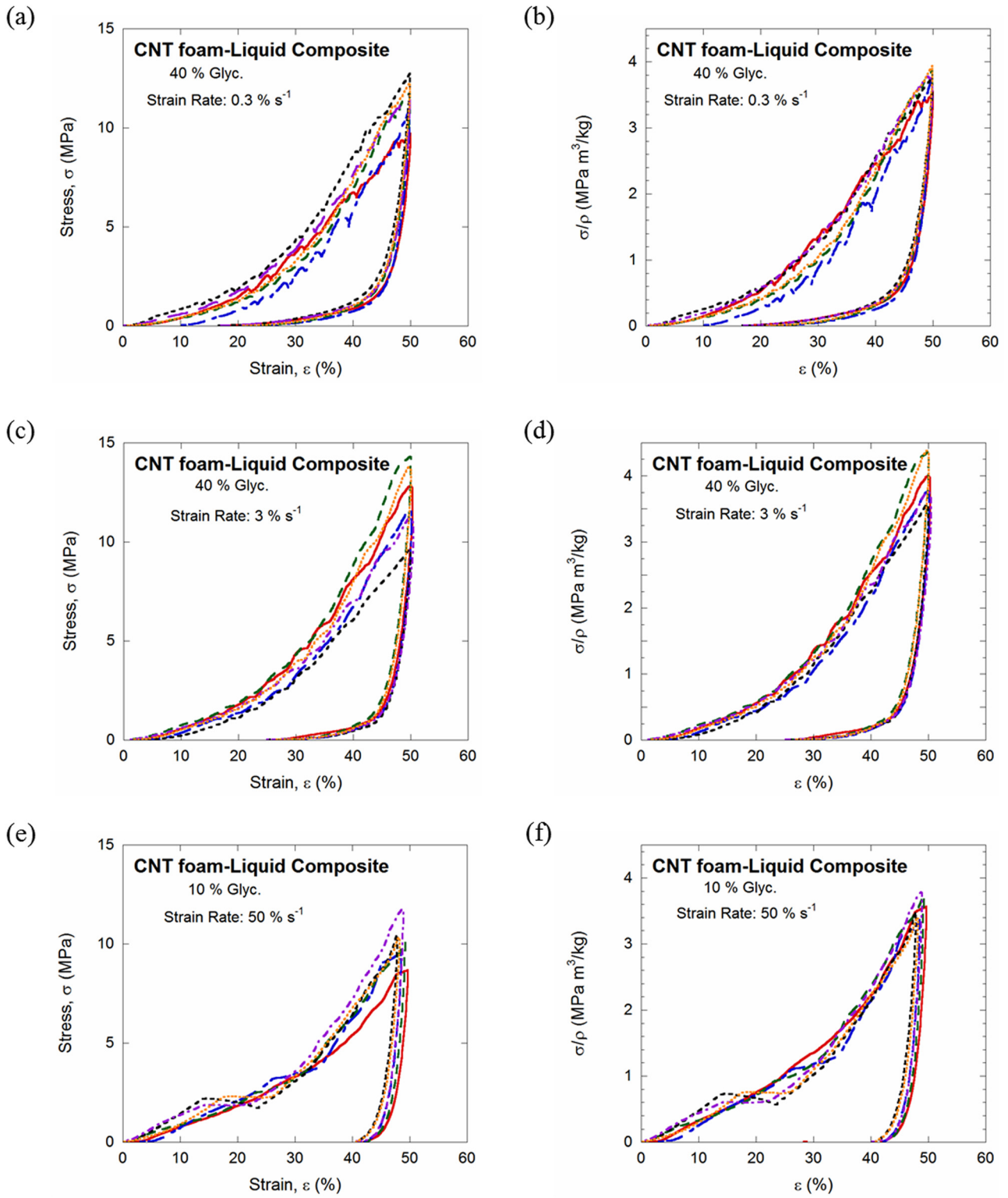

FIG. 2. Typical stress-strain plots of fluid-impregnated CNT foams. (a), (c), and (e) Show the raw stress-strain data, whereas (b), (d), and (f) show the corresponding strains plotted as a function of the normalized stress. Stress-strain curves, corresponding to 6 different CNT foam-liquid composites tested under identical experimental conditions, are shown in each graph.

discussions, it can be concluded that the presence of high concentrations of glycerol inside the CNT foam drastically reduced the strength of the CNT foam-fluid composite.

In general, CNT foams derive their strength from (i) the interaction of entangled CNTs at a node (or a junction point), which acts as a pinning point against the free sliding of CNTs, (ii) the inherent CNT bending stiffness, and (iii) van der Waals' interactions between adjacent, parallel CNTs.[17,29–31] Since CNTs are hydrophobic,[4] pure water cannot easily penetrate between adjacent, closely spaced CNTs and does not affect the CNT foams' strength. However, glycerol has moderately high affinity to CNTs and wets the foams much better as compared to water.[32] Adding glycerol into the solution enhances capillary forces and allows the liquid to penetrate more effectively between the closely spaced CNTs. This significantly reduces van der Waals' interactions

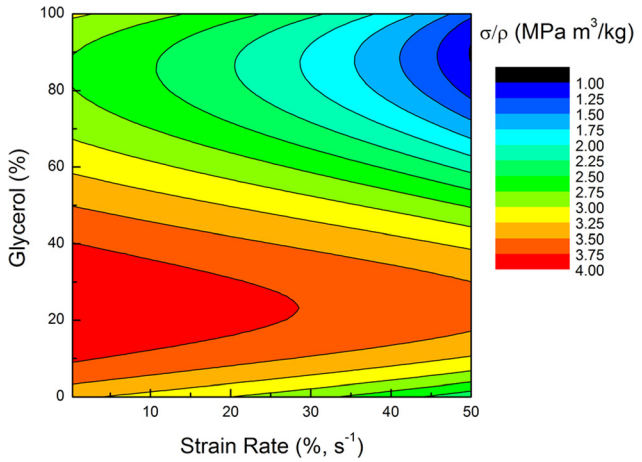

FIG. 3. Contour plot showing the variation of normalized stress at a strain of 50% as a function of the strain rate and the glycerol concentration in the water-glycerol solution. The stress was normalized dividing it by the density of the as-grown, dry CNT foam.

between adjacent CNTs, and therefore reduces the strength of the CNT foam. This argument is consistent with the observations in our experiments as well as the literature.[33] Based on the above argument, and the fact that van der Waals' force is directly proportional to Hamakar constant, which then scales with the interaction area between the adjacent bodies,[33] the resistance to deformation due to van der Waals' interaction can be phenomenologically given as

$$\sigma_{vdW} = C_1(A - A_w) = C_1\left(A - \alpha v_f^n\right) = K - V v_f^n, \quad (1)$$

where σ is the resistive stress, subscript *vdW* represents van der Waals' interaction, C_1 is a constant, A is the initial area of CNT bundles adjacent to each other, and A_w is the area of CNT bundles wetted by the liquid. A_w will monotonically increase with the volume fraction of the wetting liquid glycerol, v_f and, in Eq. (1), it is assumed to increase following a power law with an exponent of n and a coefficient of α. Here, K and V are constants representing the van der Waals interaction between adjacent CNT bundles in the dry state, and the effectiveness of the confined wetting liquid in decreasing the van der Waals' interaction, respectively. Since K depends on the initial overlap area between CNT bundles (i.e., A), it scales with the density of the CNT foams, and contributes to the effect of the density on the strength of CNT foams as mentioned earlier (Fig. 2) and reported previously.[9,27] Therefore, since all CNT foams tested in this study were fabricated in the same batch, the contribution of K in the variation of normalized stress (i.e., σ/ρ) may be neglected for the CNT foams tested at a given strain rate. Furthermore, since glycerol was the only wetting liquid used in this study, the effect of penetration of the wetting liquid on the van der Waals interaction should also remain the same for different solutions used in this study. Thus, the effect of V on σ/ρ can be assumed to be independent of v_f.

Another aspect of the liquid impregnated CNT foam composite under compression loading is the outward flow of the liquid from the pores of the CNT foam. For Newtonian fluid and under quasi-static loading condition, the component of stress arising from the outward flow of the liquid can be assumed to be given by Darcy's law[25]

$$\sigma_{L-OF} = C_2 \dot{\varepsilon} \eta, \quad (2)$$

where subscript *L-OF* represents liquid outward flow, C_2 is a constant dependent on the permeability of CNT foam, η is the viscosity of the liquid, and $\dot{\varepsilon}$ is the applied strain rate. Since the viscosity of a water-glycerol solution can be given as $H\exp(2.9v_f)$, where H is a constant,[34] Eq. (2) can be rewritten as follows:

$$\sigma_{L-OF} = C_2 \dot{\varepsilon} H \exp(2.9v_f) = D\exp(2.9v_f). \quad (3)$$

Here, D is the product of C_2, H, and the strain rate, and it is a constant for a fixed strain rate.

Now, assuming I to be the inherent stiffness of the CNT foam, deriving its value from node strength, bending stiffness of the individual CNT bundles, etc., Eqs. (1) and (3) give the following expression for the stress for a CNT foam-liquid composite:

$$\sigma = S + D\exp(2.9v_f) - V v_f^n, \quad (4)$$

where $S = I + K$. The second term in right hand side represents the strengthening due to the liquid (i.e., outward flow) whereas the third term represents the loss in the strength of CNT foam due to the decrease in the van der Waals' interaction between the adjacent CNT strands. Equation (4) assumes that the effects of the outward flow of the liquid from the foam and the entanglement of CNT bundles due to wetting by liquid linearly superimpose and these two processes do not affect each other.

Figure 4 shows the best curve fit analysis of the experimental data on the variation of the strength of the composite with the glycerol concentration in the water-glycerol solution at various strain rates. On the right, the values of the constants S, D, V, and n at different strain rates are listed. The curve fit parameter, R, is also provided. The constant S, which represents the strength of the CNT foam structure arising from the inherent stiffness of CNT bundles (I) and van der Waals interaction between adjacent CNT bundles (K), decreased with the strain rate; however, the decrease was slower at the smaller strain rates and was rapid at the highest

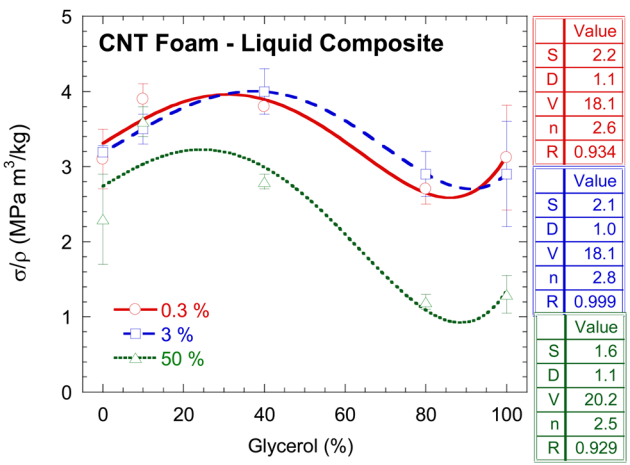

FIG. 4. Best-fit curve analysis of the experimental data using Eq. (4). The tables on the right show the values of various constants calculated from the curve fit analysis at different strain rates.

strain rate (50% s^{-1}) used in this study. A close inspection of Figure 4 reveals that the variation of S with the strain rate is similar to variation of stress at 50% strain of the as-grown, dry CNT samples. The value of constant V remained stationary at low strain rates; however, it noticeably increased at high strain rate suggesting a dramatic increase in the confinement of the wetting liquid inside a CNT cell only at high strain rates. The constant n did not systematically depend on the strain rate and its value remained close to 2.5; this indicates that n, which represents the static configuration of CNT-liquid composite, as expected, does not depend on the applied strain rate. Interestingly, these experiments do not show effect of strain rate on D (arising from Darcy's Law) suggesting a dynamic change in the permeability of CNT foam with the strain rate. One of the implications of this observation is increase in the pore size with strain rate. This is possible if the increase in the confinement of the wetting liquid inside a CNT cell at higher strain rate caused more dilation of the foam structure, which is consistent with the earlier proposal of the decrease in the tightly bonded areas between CNT bundles with an increase in their wetting by glycerol (as well as also with the variation of constant V with strain rate). Although Eq. (4) is a phenomenological relationship, it aptly captures the fundamentals of the deformation behavior of CNT foam in a solution of a CNT-phobic and a CNT-wetting liquid.

The effect of strain rate and fluid concentrations on the compressive behavior of CNT foams impregnated with water-glycerol solution, a Newtonian fluid, was studied. At lower strain rates, the presence of fluid played a minimal role in determining the overall mechanical response of the foam; however, the confined fluid played an important role in reducing the frictional interaction between CNTs both at high strain rates and when the glycerol concentration was very high. The wetting of CNTs by glycerol, which readily occurred in solution with high glycerol concentration and at high strain rates, reduced the van der Waals' interaction between CNT strands; this resulted in a reduction in the load bearing capacity of the CNT foam-liquid composite. An optimum concentration of glycerol in the water-glycerol solution (or viscosity of liquid) was observed where the CNT foam-liquid composite showed relatively high load bearing capacity (and the energy absorption per cycle), especially at low strain rates.

This work was partially supported by the Institute for Collaborative Biotechnologies, under Contract No. W911NF-09-D-0001 with the Army Research Office.

[1]J. M. Schnorr and T. M. Swager, Chem. Mater. **23**, 646 (2011).
[2]A. Cao, P. L. Dickrell, W. G. Sawyer, M. N. Ghasemi-Nejhad, and P. M. Ajayan, Science **310**, 1307 (2005).
[3]K. Mylvaganam and L. C. Zhang, Appl. Phys. Lett. **89**, 123127 (2006).
[4]S. Kaur, P. M. Ajayan, and R. S. Kane, J. Phys. Chem. B **110**, 21377 (2006).
[5]A. A. Zbib, S. D. Mesarovic, E. T. Lileodden, D. McClain, J. Jiao, and D. F. Bahr, Nanotechnology **19**, 175704 (2008).
[6]M. A. Worsley, S. O. Kucheyev, J. H. Satcher, A. V. Hamza, and T. F. Baumann, Appl. Phys. Lett. **94**, 073115 (2009).
[7]A. Misra, J. R. Greer, and C. Daraio, Adv. Mater. **21**, 334 (2009).
[8]P. D. Bradford, X. Wang, H. Zhao, and Y. T. Zhu, Carbon **49**, 2834 (2011).
[9]A. Misra, J. R. Raney, A. C. Craig, and C. Daraio, Nanotechnology **22**, 425705 (2011).
[10]Y. Gao, T. Kodama, Y. Won, S. Dogbe, S. Pan, and K. E. Goodson, Carbon **50**, 3789 (2012).
[11]V. V. Shastry, U. Ramamurty, and A. Misra, Carbon **50**, 4373 (2012).
[12]L. Lattanzi, J. R. Raney, L. De Nardo, A. Misra, and C. Daraio, J. Appl. Phys. **111**, 074314 (2012).
[13]J. R. Raney, F. Fraternali, and C. Daraio, Nanotechnology **24**, 255707 (2013).
[14]M. S. Kiran, U. Ramamurty, and A. Misra, Nanotechnology **24**, 015707 (2013).
[15]H. Radhakrishnan, S. D. Mesarovic, A. Qiu, and D. F. Bahr, Int. J. Solids Struct. **50**, 2224 (2013).
[16]J. R. Raney, A. Misra, and C. Daraio, Carbon **49**, 3631 (2011).
[17]A. Misra, J. R. Raney, L. De Nardo, A. E. Craig, and C. Daraio, ACS Nano **5**, 7713 (2011).
[18]J. R. Raney, F. Fraternali, A. Amendola, and C. Daraio, Compos. Struct. **93**, 3013 (2011).
[19]X. Yu, R. Rajamani, K. A. Stelson, and T. Cui, Sens. Actuators, A **132**, 626 (2006).
[20]R. Chowdhury, S. Adhikari, and J. Mitchell, Physica E **42**, 104 (2009).
[21]X. Gui, J. Wei, K. Wang, A. Cao, H. Zhu, Y. Jia, Q. Shu, and D. Wu, Adv. Mater. **22**, 617 (2010).
[22]M. Warner and S. F. Edwards, Europhys. Lett. **5**, 623 (1988).
[23]M. A. Dawson, G. H. Mckinley, and L. J. Gibson, J. Appl. Mech. **75**, 041015 (2008).
[24]M. A. Dawson, G. H. Mckinley, and L. J. Gibson, J. Appl. Mech. **76**, 061011 (2009).
[25]L. J. Gibson and M. F. Ashby, *Cellular Solids: Structure and Properties*, 2nd ed. (Cambridge University Press, 1997).
[26]N. N. Cheng, Ind. Eng. Chem. Res. **47**, 3285 (2008).
[27]A. Qiu and D. F. Bahr, Carbon **55**, 335 (2013).
[28]S. K. Reddy, A. Suri, and A. Misra, Appl. Phys. Lett. **102**, 241919 (2013).
[29]F. W. Delrio, M. P. De Boer, J. A. Knapp, E. D. Reedy, P. J. Clews, and M. L. Dunn, Nature Mater. **4**, 629 (2005).
[30]A. A. Kuznetsov, A. F. Fonseca, R. H. Baughman, and A. A. Zakhidov, ACS Nano **5**, 985 (2011).
[31]A. F. Gilvaei, K. Hirahara, and Y. Nakayama, Carbon **49**, 4928 (2011).
[32]L. A. Bulavin, N. I. Lebovka, Yu. A. Kyslyi, S. V. Khrapatyi, A. I. Goncharuk, I. A. Mel'nyk, and V. I. Koval'chuk, Ukr. J. Phys. **56**, 217 (2011), available at http://ujp.bitp.kiev.ua/files/journals/56/3/560302p.pdf.
[33]P. P. S. S. Abadi, M. R. Maschmann, S. M. Mortuza, S. Banerjee, J. W. Baur, S. Graham, and B. A. Cola, Carbon **69**, 178 (2014).
[34]See supplementary material at http://dx.doi.org/10.1063/1.4881843 for the derivation of the expression for viscosity of water-glycerol mixture as a function of glycerol concentration.